Soils and Foundations 2013;53(6):868–878

The Japanese Geotechnical Society

Soils and Foundations

www.sciencedirect.com
journal homepage: www.elsevier.com/locate/sandf

# Effects of fines and water contents on the mechanical behavior of interlayer soil in ancient railway sub-structure

Trong Vinh Duong[a], Anh Minh Tang[a], Yu-Jun Cui[a,*], Viet Nam Trinh[a], Jean-Claude Dupla[a], Nicolas Calon[b], Jean Canou[a], Alain Robinet[b]

[a]*Ecole des Ponts ParisTech, Laboratoire Navier/CERMES, 6-8 av. Blaise Pascal, Cité Descartes, Champs-sur-Marne, 77455 Marne-la-Vallée, cedex 2, France*
[b]*French National Railway Company (SNCF), France*

Received 25 March 2013; received in revised form 31 July 2013; accepted 25 August 2013
Available online 20 November 2013

**Abstract**

In the ancient railway sub-structure in France, after years of operation, the inter-penetration of fine particles of sub-grade and ballast has created a new layer referred to as the interlayer. As it was naturally formed, the fines content and water content of the interlayer vary considerably. In this study, the effects of the fines and water contents on the mechanical behavior of interlayer soil were investigated by carrying out large-scale monotonic and cyclic triaxial tests. The results of the monotonic triaxial tests show that adding more fines in the interlayer soil does not significantly change the shear strength in the dry condition (water content $w=4\%$ and 6%), but drastically decreases the shear strength parameters (friction angle and cohesion) in the nearly saturated condition ($w=12\%$). The cyclic triaxial tests were performed at various deviator stress levels. By considering the permanent axial strain at the end of application of each stress level, it was found that the higher the fines content in the nearly saturated condition ($w=12\%$), the larger the permanent axial strain. In the case of lower water content ($w=4\%$ and 6%), the opposite trend was identified: adding fines decreases the permanent axial strain.


*Keywords:* Railway sub-structure; Interlayer; Fine particles; Water content; Triaxial test; Permanent strain; IGC; D06

## 1. Introduction

In France, even though some new railway lines for high speed train have been constructed since 1970s, ancient lines (most of which were constructed in the 1800s) still represent 94% of the 30,000 km total network. While the new railway sub-structures are composed of several layers (ballast, sub-ballast, capping layer, etc.) whose characteristics and functions are well defined, this is not the case for the ancient ones, which consist mainly of ballast emplaced directly on natural sub-grade at the moment of construction. Under train action over years, the inter-penetration between ballast and sub-grade fine particles created a new layer, which is referred to as the interlayer (Calon et al., 2010; Trinh, 2011; Duong et al., 2013).

The presence of fines inside ballast is known as one of the main causes of fouling (Ayres, 1986; Selig and Waters, 1994; Alobaidi and Hoare, 1998a; 1998b; 1999; Indraratna and Salim, 2002; Voottipruex and Roongthanee, 2003; Ghataora et al., 2006; Mayoraz et al., 2006; Zeghal, 2009; Giannakos, 2010; Lieberenz and Piereder, 2011; Indraratna et al., 2011a, 2011b; Bailey et al., 2011; Read et al., 2011; Sussmann et al., 2012). Fouled ballast is usually considered as a detriment to

*Corresponding author. Tel.: +33 1 64 15 35 50; fax: +33 1 64 15 35 62.
*E-mail address:* yujun.cui@enpc.fr (Y.-J. Cui).
Peer review under responsibility of The Japanese Geotechnical Society.

Production and hosting by Elsevier

0038-0806 © 2013 The Japanese Geotechnical Society. Production and hosting by Elsevier B.V. All rights reserved.
http://dx.doi.org/10.1016/j.sandf.2013.10.006

sub-structures which needs to be replaced in practice. However, the interlayer can be maintained during the renewal of ancient tracks mainly due to its good bearing capacity. As the interlayer is naturally formed, the fines nature and fines content vary considerably. In addition, the water content in the interlayer can change significantly depending on the weather conditions. From a practical point of view, it is important to assess the effect of the fines content and water content on the permanent strain of interlayer under cyclic loading.

The important role of water content in the mechanical behavior of sub-structures has been shown in numerous studies: when water is entrapped in the sub-structure, pore pressure can increase significantly under the train, resulting in a decrease in both the shear strength and stiffness of sub-structures (Alobaidi and Hoare, 1994, 1996; Huang et al., 2009; Indraratna et al., 2011b; Trinh et al., 2012). Various studies have also shown the significant influence of fines content: increasing the quantity of fines significantly affects the mechanical behavior of coarse-grained materials (Babic et al., 2000; LCPC and SETRA, 2000; Pedro, 2004; Naeini and Baziar, 2004; Kim et al., 2005; Verdugo and Hoz, 2007; Cabalar, 2008, 2011; Seif El Dine et al., 2010; Ebrahimi, 2011; Anbazhagan et al., 2011). It has been observed that if the fines content reaches a critical value, the soil behavior changes completely. However, it seems that there is no unique threshold of fines content for all kinds of soil, suggesting that the influence of fines content depends on the soil nature.

On the whole, for the railway sub-structures, the combined effect of water content and fines content has been scarcely studied. In this study, the effects of water content and fines content are investigated by performing large-scale monotonic and cyclic triaxial tests on interlayer soil specimens prepared by compaction at three water contents and four fines contents. The mechanical properties such as friction angle, cohesion and permanent axial strain are analyzed.

## 2. Materials

Interlayer soil was taken from the site of Sénissiat, near Lyon, France. The interlayer has a thickness of about 0.3 m. The grain size distribution curves of the interlayer soil ($ITL_0$) and the sub-grade ($SG$) are presented in Fig. 1. Mineralogical analysis showed that the interlayer soil is a mixture of materials that came from the construction of the track, the maintenance (broken stones, gravel, sand, etc.), the aging process of track components and the sub-grade. The density of soil particles smaller than 2 mm is $\rho_s = 2.67$ Mg/m$^3$. For the soil particles larger than 2 mm and those greater than 20 mm, the value is $\rho_s = 2.68$ Mg/m$^3$. More details about the characterization of this soil can be found in Trinh (2011) and Trinh et al. (2010a, 2010b, 2011a, 2011b).

In order to study the influence of fines content on the mechanical behavior of interlayer soil, the fines content was varied by decreasing or increasing the sub-grade fraction: $-10\%$ ($ITL_{-10}$), $+5\%$ ($ITL_5$) and $+10\%$ ($ITL_{10}$) by dry mass (dry mass of sub-grade/dry mass of interlayer soil). Note that unlike in the case of fouled ballast where fouling material is defined as the portion passing through 9.5 mm sieve (Selig and Waters, 1994), as the interlayer was created mainly by the interpenetration of ballast and sub-grade, the sub-grade was considered as fines in the interlayer when changing the fines contents. As the sub-grade consist mainly of fine particles smaller than 80 μm (see Fig. 1), $ITL_{-10}$ was prepared by removing a certain quantity of particles smaller than 80 μm from the natural interlayer soil by sieving. $ITL_5$ and $ITL_{10}$ were prepared simply by adding the mass of sub-grade required. The grain size distribution curves of $ITL_{-10}$, $ITL_5$ and $ITL_{10}$ are also shown in Fig. 1.

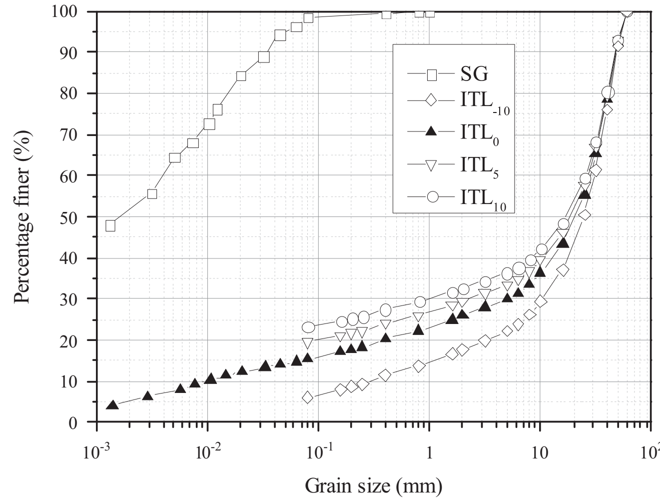

Fig. 1. Grains size distribution of the studied soils.

Basically, the effect of fines on the mechanical behavior of interlayer soil is similar to that on fouled ballast; thereby, some parameters used to characterize the fouling state of ballast can be adopted for the interlayer soil. Selig and Waters (1994) proposed the fouling index ($FI$) to describe the ballast fouling based on the gradation obtained from representative specimens in North-America, as follows:

$$FI = P_4 + P_{200} \tag{1}$$

where $P_4$ and $P_{200}$ are percentages of ballast particles passing through sieve N° 4 (4.75 mm) and N° 200 (0.075 mm), respectively.

The Relative Fouling Ratio ($R_{b-f}$), proposed by Indraratna et al. (2011b), describes the weighted ratio of the dry mass of fouling particles $M_f$ (passing through 9.5-mm sieve) to the dry mass of ballast $M_b$ (particles retained in 9.5-mm sieve):

$$R_{b-f} = \frac{M_f \times (G_{s-b}/G_{s-f})}{M_b} \times 100\% \tag{2}$$

where $G_{s-f}$, $G_{s-b}$ are specific densities of fouling materials and ballast, respectively.

Using these two parameters, the fouling states of $ITL_{-10}$, $ITL_0$, $ITL_5$ and $ITL_{10}$ were evaluated, and the results are presented in Table 1. It can be seen that only $ITL_{-10}$ is in the category of "*fouled*" while the other three materials fall in the category of "*highly fouled*". Note that the values divided these two categories are 39 for $FI$ and 50 for $R_{b-f}$.

Table 1
Fouling state of the materials studied.

| Soil | Fouling index $FI$ (−) | Relative fouling ratio $R_{b-f}$ (%) | Fouling category |
|---|---|---|---|
| | 35 | 40 | *Fouled* |
| $ITL_0$ | 45 | 56 | *Highly fouled* |
| $ITL_5$ | 52 | 64 | *Highly fouled* |
| $ITL_{10}$ | 59 | 72 | *Highly fouled* |

## 3. Experimental procedure

All the soil specimens were prepared before being subjected to triaxial tests. The specimens were prepared by oven-drying for 24 h before water was added using a large mixer to reach the target water contents. The wet materials were then stored in hermetic containers for at least 24 h for moisture homogenization. Compaction was performed using a vibrating hammer. This procedure of sample preparation follows the French standard (AFNOR, 2005) and was used by Trinh et al. (2012). All the tested specimens were prepared at a dry unit mass of 2.01 Mg/m$^3$. This is the maximum dry density which can be reached in the adopted condition. To test this interlayer soil with the largest particles whose diameter can reach 60 mm, a large-scale triaxial device developed by Dupla et al. (2007) was used allowing testing specimens of 300 mm in diameter and 600 mm in height. A schematic view of the triaxial apparatus was presented in Fig. 2. A vertical displacement was integrated in the hydraulic actuator giving the axial deformation. A second external hydraulic actuator generates the confining water pressure $\sigma_3$. The change of water volume allows the volumetric strain $\varepsilon_v$ to be determined.

Both monotonic and cyclic triaxial tests can be carried out. In the case of cyclic tests, large number of cycles (up to several millions) at a frequency of several tens of Hertz (depending on the displacement amplitude) can be applied.

In order to determine the shear strength parameters of interlayer soil (friction angle and cohesion), monotonic drained triaxial tests were first performed on $ITL_0$ and $ITL_{10}$ at two different water contents and under different confining pressures. Some studies with triaxial tests on other similar materials under different confining pressures were performed by Taheri and Tatsuoka (2012) and Vilhar et al. (2013). To investigate the permanent strain development under cyclic loading, cyclic triaxial tests were conducted on all soils at three different water contents. The experimental program is presented in Table 2 for the monotonic triaxial tests and in Table 3 for the cyclic triaxial tests. The tests are named according to the material ($ITL_{-10}$, $ITL_0$, $ITL_5$, $ITL_{10}$), water content and confining pressure. For instance, $ITL_0w4s30$ means a monotonic triaxial test on $ITL_0$ at 4% water content and 30 kPa confining pressure; $ITL_0w4C$ means a cyclic triaxial test on $ITL_0$ at 4% water content.

In the cyclic triaxial tests, the multi-step loading procedure proposed by Gidel et al. (2001) was adopted. This procedure allows several stress levels to be applied before the soil specimen reaches failure state, reducing thus the number of tests and avoiding the variability of soil specimens. After the specimen was installed, a confining pressure $\sigma_3 = 30$ kPa was applied. The choice of the stress levels was based on the stress distribution in the railway platform as well as the envelope of shear strength determined from the monotonic triaxial tests. Note that the stress distribution within the interlayer depended on the wheel load, dimensions of sleeper, thickness of ballast layer. In the case of France, the wheel load applied by a train is about 16–22 t per axle

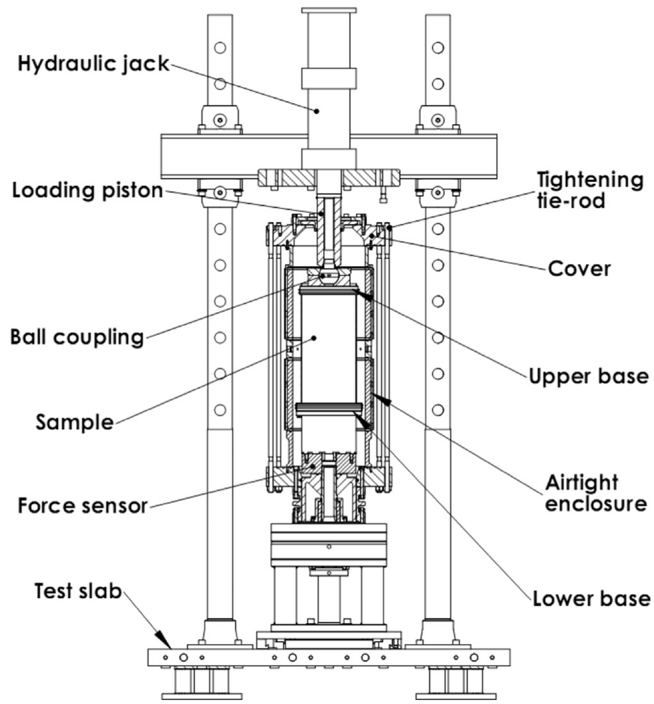


Fig. 2. Schematic view of the large triaxial apparatus (Trinh et al. 2012).

Table 2
Program of monotonic triaxial tests.

| Water content (%) | Confining pressure (kPa) | Soil | |
|---|---|---|---|
| | | $ITL_0$ | $ITL_{10}$ |
| $w=4$ | 30 | $ITL_0w4s30$ | $ITL_{10}w4s30$ |
| | 100 | $ITL_0w4s100$ | $ITL_{10}w4s100$ |
| | 200 | $ITL_0w4s200$ | $ITL_{10}w4s200$ |
| | 400 | $ITL_0w4s400$ | – |
| $w=12$ | 100 | $ITL_0w12s100$ | $ITL_{10}w12s100$ |
| | 200 | – | $ITL_{10}w12s200$ |
| | 400 | $ITL_0w12s400$ | – |

Table 3
Program of cyclic triaxial tests.

| Water content (%) | Soil | | | |
|---|---|---|---|---|
| | $ITL_{-10}$ | $ITL_0$ | $ITL_5$ | $ITL_{10}$ |
| $w=4$ | $ITL_{-10}w4C$ | $ITL_0w4C$ | – | $ITL_{10}w4C$ |
| $w=6$ | $ITL_{-10}w6C$ | $ITL_0w6C$ | $ITL_5w6C$ | $ITL_{10}w6C$ |
| $w=12$ | $ITL_{-10}w12C$ | $ITL_0w12C$ | – | $ITL_{10}w12C$ |

(Alias, 1984); the thickness of ballast and interlayer varies from 250 mm to 600 mm and the distance between two sleepers is 0.6 m. Based on the elasticity theory, the vertical stress at the top of interlayer can be calculated: 40–90 kPa. This range is similar to that observed for Indian railways (Jain and Keshav, 1999) and American railways (Selig and Waters, 1994; Yang et al., 2009). Considering a Poisson's ratio of 0.3–0.4 as proposed by Selig and Waters (1994), an average value of 30 kPa can be estimated for the horizontal stress. Note however that in other countries where heavier wagons are used the wheel load may reach 30 t per axle (Alias, 1984), corresponding to a vertical stress of 120–140 kPa on the interlayer (Li and Selig, 1998; Jain and Keshav, 1999; Grabe and Clayton, 2009). In this study, a maximum vertical stress of 200 kPa was applied in the cyclic triaxial tests.

During the cyclic tests, the maximum deviator stress ($q_{max}$) was increased in steps (from 0 to various desired values) while the confining pressure was kept constant. The specimens were loaded to 30,000 cycles at a frequency of 5 Hz for each maximum deviator stress level. The frequency considered is the dominant one among a number of frequencies generated in the French ancient sub-structures at a train speed of 100 km/h (SNCF, 2009). For $ITL_{-10}$, $ITL_0$ and $ITL_{10}$, the specimens were loaded at three water contents ($w=4\%$; 6% and 12%), corresponding to three initial degrees of saturation ($S_{ri}=32\%$; 49% and 100%). In the case of $ITL_5$, because of lack of material, only one cyclic test at a water content of $w=6\%$ was conducted.

## 4. Results and discussion

### 4.1. Monotonic triaxial test

The results of monotonic triaxial tests on $ITL_0$ and $ITL_{10}$ at two water contents ($w=4\%$ and 12%) and under different confining pressures are presented in Figs. 3–6. Dilation is considered as negative and compression is positive. On the whole, with higher confining pressure, the peak deviator stress was higher and the contractive behavior was more significant, as expected.

For $ITL_0$, under 400 kPa confining pressure, the behavior is merely contractive (Fig. 3b) and no peak deviator stress was observed till 12% of axial deformation (Fig. 3a) in the cases of water content $w=4\%$ and 12%. However, it is possible that peak deviator stress would have appeared at a larger axial

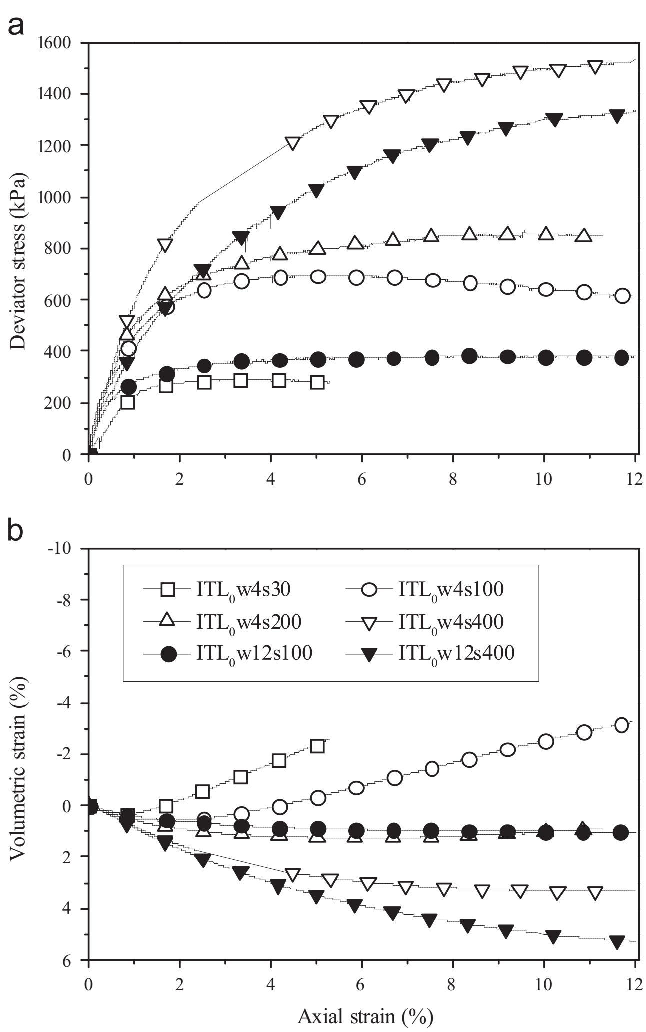


Fig. 3. Results from monotonic triaxial tests on $ITL_0$ – effect of water content.

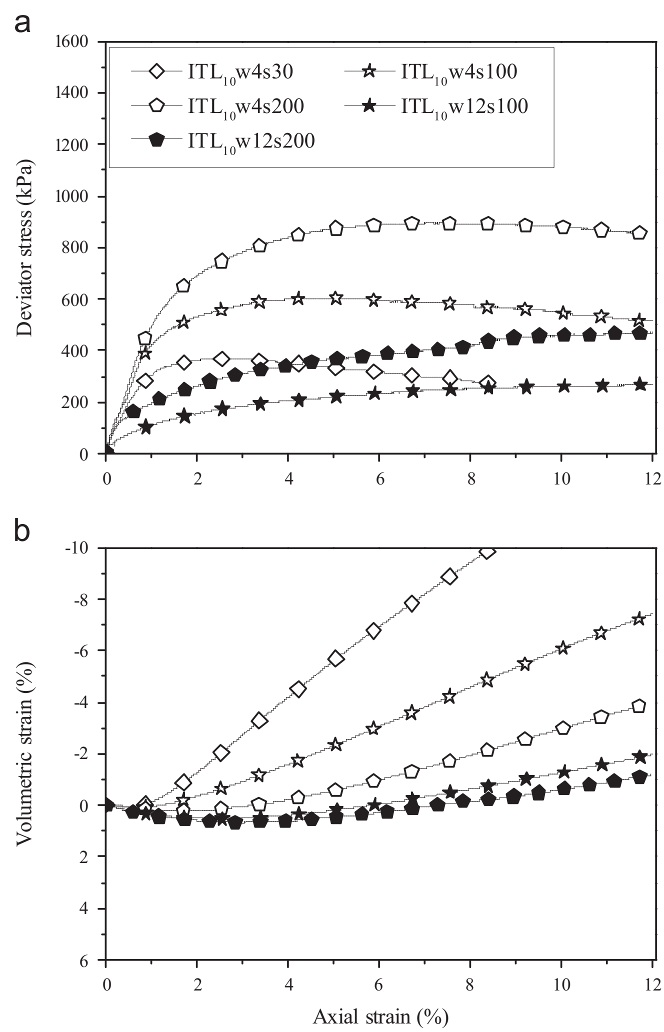


Fig. 4. Results from monotonic triaxial tests on $ITL_{10}$ – effect of water content.

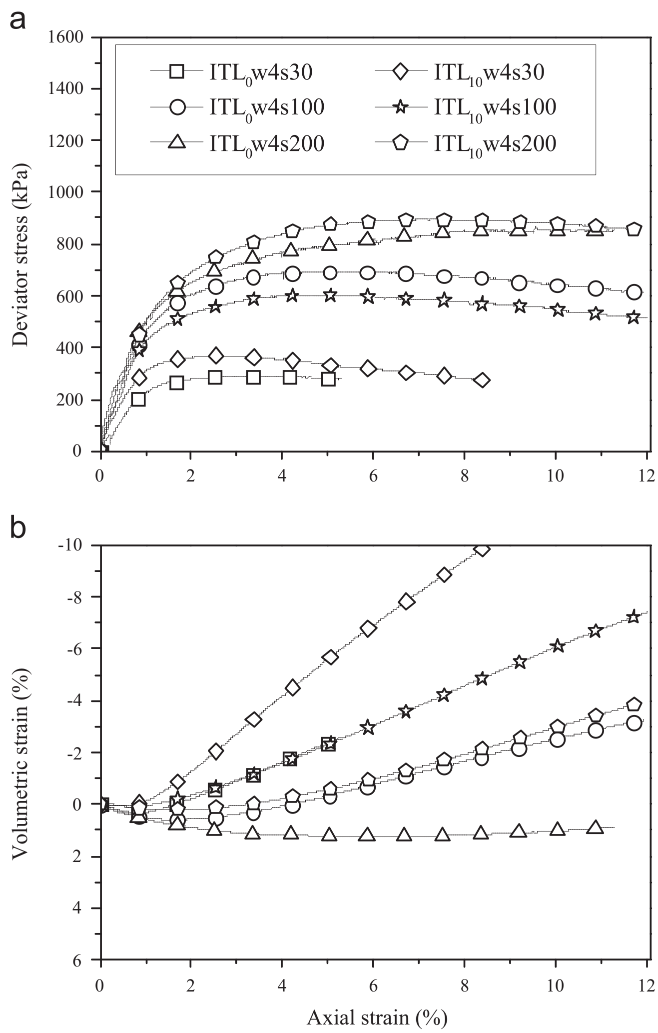


Fig. 5. Results from monotonic triaxial tests on $ITL_0$ and $ITL_{10}$ at $w=4\%$ – effect of fine particles content.

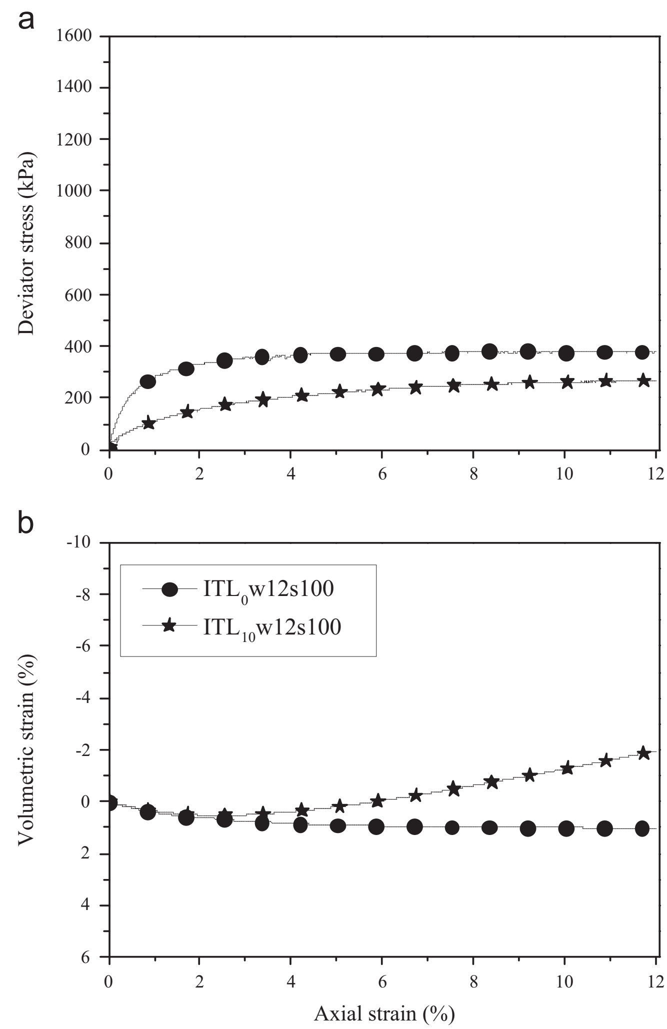


Fig. 6. Results from monotonic triaxial tests on $ITL_0$ and $ITL_{10}$ at $w=12\%$ – effect of fines content.

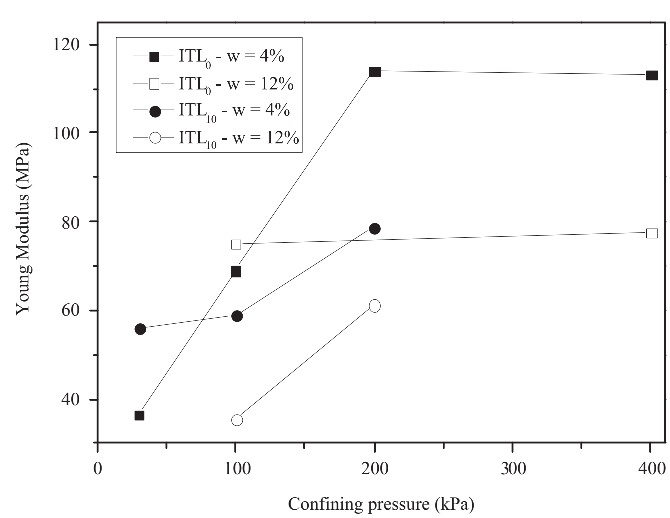


Fig. 7. Young modulus versus confining pressure for $ITL_0$ and $ITL_{10}$ at $w=4\%$ and 12%.

strain. Indeed, previous studies on ballast shear behavior showed that the peak value can be recorded at an axial strain beyond 12% (Indraratna et al., 1998). Under 100 kPa confining pressure and at $w=4\%$, a peak deviator stress was recorded, and the volume change behavior was first contractive then dilative. On the contrary, at the saturated state ($w=12\%$) the peak deviator stress was not recorded and the behavior was solely contractive. As mentioned before, it is possible that peak deviator stress would have appeared at a larger axial strain. This effect of water content on the ductility/fragility was also identified by Cui and Delage (1996) for a compacted unsaturated silt.

For $ITL_{10}$ (Fig. 4), whatever the water content and the confining pressure, the volume change behavior is clearly characterized by contraction followed by dilatancy. However, increasing water content from $w=4\%$ to 12% favorites the compression behavior (Fig. 4b). In Fig. 4a, peak deviators were recorded at $w=4\%$ but not at $w=12\%$, showing again the effect of water content on the ductility/fragility of soil.

The effect of fines content can be appreciated in Figs. 5 and 6 for $w$=4% and 12%, respectively. Under the unsaturated condition ($w$=4%), adding more fines increases the deviator stress or shear strength in the test with $\sigma_3$=30 kPa and 200 kPa but decreases in the test with $\sigma_3$=100 kPa (Fig. 5a). The decrease under 100 kPa confining pressure is difficult to explain and further study is needed to clarify this point. Note that this particularity does not affect the overall interpretation thanks to the data with other three confining pressures (30, 200 and 400 kPa). With regard to volumetric strain, the increase of fines content makes the compression more pronounced (Fig. 5b). This phenomenon can be explained as follows: the fine particles are normally more compressible than the big solid grains. The compression of specimen becomes more significant when the big particles were replaced by fine particles. At nearly saturated state ($w=12\%$), adding fines makes the volume change more dilative (Fig. 6a). In Fig. 6a, the curve of $ITL_0$ is always above the curve of $ITL_{10}$, showing that addition fines decreases the shear strength. The different effect of fines content on shear strength between $ITL_0$ and $ITL_{10}$ can be explained by both the suction and fines effects. In unsaturated state, for the same water content, increasing fines content makes the suction higher, thus strengthening the soil. On the contrary, in saturated state, suction becomes zero and the shear strength decreases accordingly.

Table 4
Internal friction angle and cohesion of studied materials.

| Water content (%) | Soil | Internal friction angle $\varphi$ (deg) | Cohesion $c$ (kPa) |
|---|---|---|---|
| $w=12$ | $ITL_0$ | 37 | 16 |
| | $ITL_{10}$ | 29 | 21 |
| $w=4$ | $ITL_0$ | 39 | 42 |
| | $ITL_{10}$ | 37 | 48 |

Fig. 7 shows the Young modulus determined in the range from 0% to 0.1% of axial strain. It can be observed that increasing confining pressure leads to an increase in the Young's modulus, with a larger rate of increase in the lower range of confining pressure (smaller than 200 kPa).

The values of internal friction angle and cohesion are determined and presented in Table 4. It can be observed that when water content increases from 4% to 12%, the values of friction angle and cohesion decrease for both $ITL_0$ and $ITL_{10}$ – the internal friction angle changes from 39° to 37° for $ITL_0$ and from 37° to 29° for $ITL_{10}$ while the cohesion decreases significantly from 42 kPa to 16 kPa for $ITL_0$ and from 48 kPa to 21 kPa for $ITL_{10}$. A similar observation about the decrease of internal friction angle when increasing water content was made by Seif El Dine et al. (2010), Indraratna et al. (2011b), Selig and Waters (1994), Fortunato et al. (2010) and Ebrahimi (2011).

The effect of fines content on shear strength can also be analyzed by fixing a water content value. In dry conditions ($w=4\%$), adding 10% of fines does not significantly change the shear strength parameters: 39° against 37° (friction angle) and 42 kPa against 48 kPa (cohesion) for $ITL_0$ and $ITL_{10}$, respectively. But in nearly saturated conditions ($w=12\%$), there is a large difference between two soils: adding fines decreases the internal friction angle from 37° to 29° and increases the cohesion from 16 kPa to 21 kPa. The test results show that the fines content has a more pronounced effect when

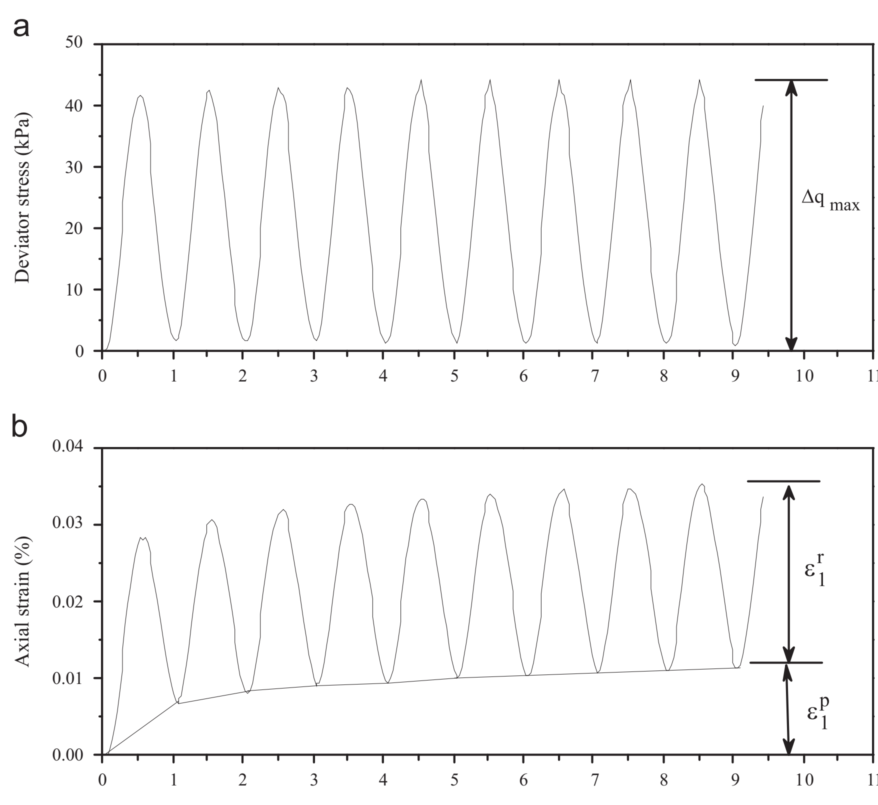


Fig. 8. First cycles of cyclic triaxial test on $ITL_0$ at $w=4\%$ (test $ITL_0$w4C) – (a) deviator stress and (b) axial strain.

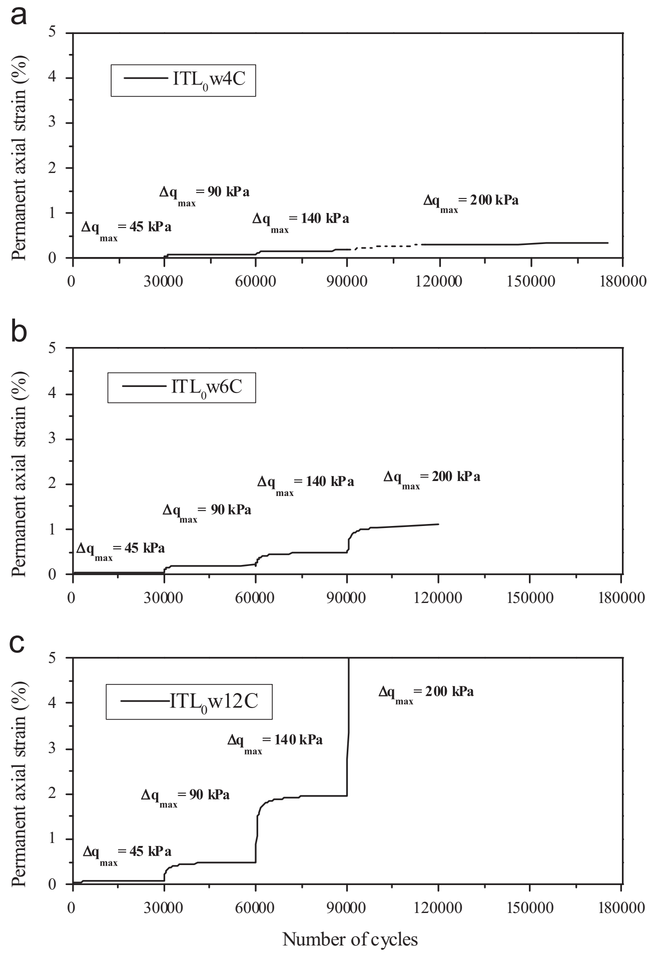


Fig. 9. Permanent axial strain versus number of cycles for $ITL_0$ – (a) 4% water content; (b) 6% water content and (c) 12% water content.

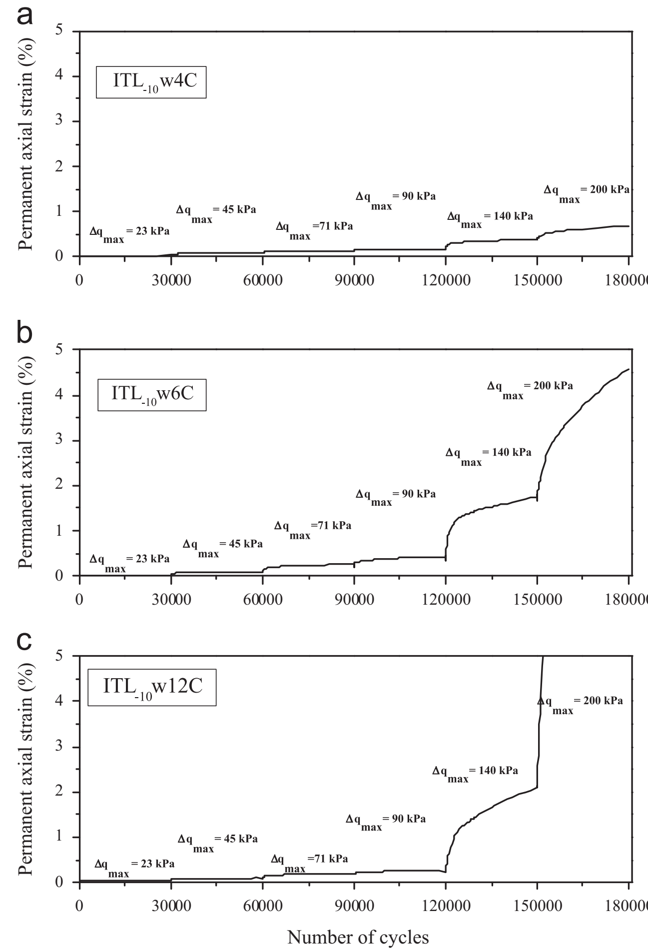


Fig. 10. Permanent axial strain versus number of cycles for $ITL_{-10}$ – (a) 4% water content; (b) 6% water content and (c) 12% water content.

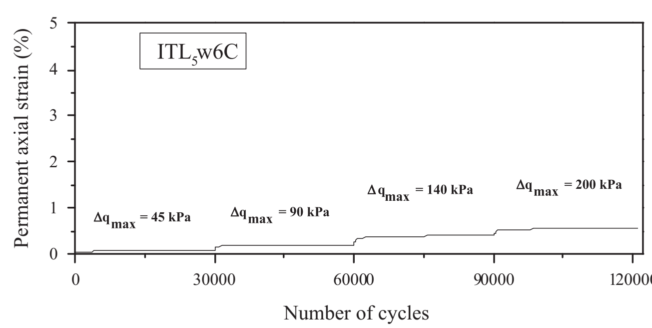


Fig. 11. Permanent axial strain versus number of cycles for $ITL_5$ at 6% water content.

the soil is close to saturation. Similar observations were made by Ebrahimi (2011), Kim et al. (2005) and Huang et al. (2009) on fouled ballast: the effects of water content and fines content are strongly related and should not be considered separately. That is, increasing water content negatively boosts the effect of fines content on shear strength parameters. The reason for the shear strength decline can be explained by the sensitivity of fines to changes of water content. In dry conditions, at given water content, thanks to the effect of suction, adding fines does not significantly change the behavior of soil. Upon water content increase, soil suction decreases, leading to a decrease in interlayer soil strength. Note that a similar suction effect was identified by Inam et al. (2012) and Wang et al. (2013).

### 4.2. Cyclic triaxial tests

The results of test $ITL_0w4C$ (for $ITL_0$ at 4% water content) are presented in Fig. 8 for the first ten cycles. The deviator stress, $q$, varies following a sinusoidal function between 0 and the maximum value, $q_{max}$=45 kPa (Fig. 8a). In Fig. 8b, two distinct parts can be identified on the axial strain curve: a reversible part, $\varepsilon_1^r$, and an irreversible part, $\varepsilon_1^p$. The reversible strain remains fairly constant, while the irreversible strain (permanent strain) increases with loading cycles, at a rate that tends to decrease with increasing number of cycles. After the stage of $q_{max}$=45 kPa, the deviator stress $q_{max}$ is then increased to 90 kPa, 140 kPa and 200 kPa. For each value of $q_{max}$, 30,000 cycles are in general applied. This number of cycles is applied for almost all loading stages except the last one in order to be able to compare the results.

In Fig. 9a, the results of test $ITL_0w4C$ are shown in terms of permanent axial strain versus number of cycles. For all deviator stress levels, the permanent axial strain increases quickly during the first cycles. It stabilizes then after 30,000 cycles at $2.19\times10^{-2}$% and $9.20\times10^{-2}$% for $q_{max}=45$ kPa and 90 kPa, respectively. At the end of stage 3 ($q_{max}=140$ kPa), the permanent axial strain is not stable after 30,000 cycles. At the last deviator stress level ($q_{max}=200$ kPa), some data was lost for the first cycles, but the test was continued until 180,000 cycles. No stabilization is observed even at this large number of cycles. In Fig. 9b and c, the results of tests $ITL_0w6C$ and $ITL_0w12C$ are presented, respectively. The trend for test $ITL_0w6C$ (for $ITL_0$ at 6% of water content) is similar to that for $ITL_0w4C$. For test $ITL_0w12C$ (near saturated state), failure is observed at $q_{max}=200$ kPa after just some limited cycles.

The variations of permanent axial strains with number of cycles for tests $ITL_{-10}$, $ITL_5$ and $ITL_{10}$ are shown in Figs. 10, 11 and 12, respectively. For $ITL_{-10}$, three tests were performed at three water contents (4%; 6% and 12%). In each test, the deviator stress was increased in steps: 23, 45, 71, 90, 140 and 200 kPa. At low stress levels (up to 90 kPa deviator stress), the permanent axial strain reaches stabilization at the end of each loading stage (30,000 cycles). By contrast, for higher stress levels (140 and 200 kPa deviator stress), the permanent axial strain continues to increase even after 30,000 cycles. For the test in near saturated state at 200 kPa deviator stress (Fig. 10c), failure is observed after some limited cycles.

In the case of $ITL_5$ (Fig. 11), only one test was performed for 6% of water content due to the limited quantity of material. Four deviator stress levels were applied (45, 90, 140 and 200 kPa). For all the stress levels, the permanent axial strain reaches stabilization at the end of loading cycles (30,000 cycles).

In the case of $ITL_{10}$ (Fig. 12), four maximum deviator stress levels of 23, 45, 71, and 102 kPa were applied for 4% and 12% of water contents. For the test of $w=6$% (Fig. 12b), the deviator stress was increased in steps from 0 to 45, to 90, 140, and 200 kPa. It can be observed that in all tests the permanent axial strain reaches stabilization at the end of loading cycles. In other words, failure did not take place.

Fig. 13 presents the permanent axial strains obtained at the end of each loading step (same number of cycles) versus the corresponding $q_{max}$ for each soil at three different water contents, allowing analyzing the effects of stress level and water content on the permanent axial strain. For $ITL_{-10}$ (Fig. 13a), the curves are similar up to 90 kPa deviator stress. Beyond 90 kPa, the permanent axial strain of $ITL_{-10}w4C$ was smaller than that of $ITL_{-10}w6C$ and $ITL_{-10}w12C$. Note that failure occurred for the nearly saturated specimen ($w=12$%) when $\Delta q_{max}=200$ kPa. For $ITL_0$ (Fig. 13b), three curves are

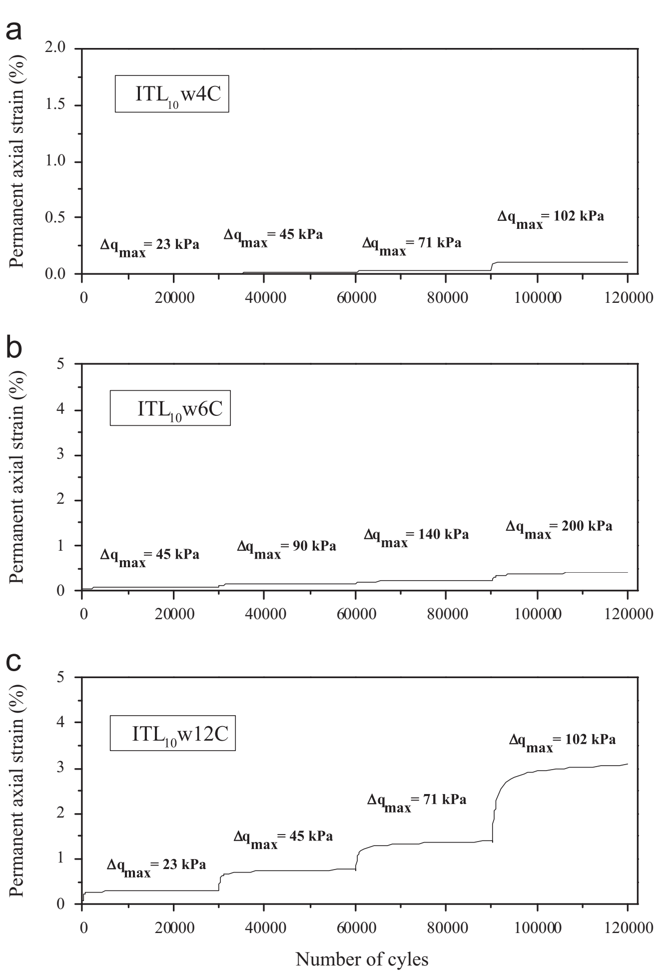


Fig. 12. Permanent axial strain versus number of cycles for $ITL_{10}$ – (a) 4% water content; (b) 6% water content and (c) 12% water content.

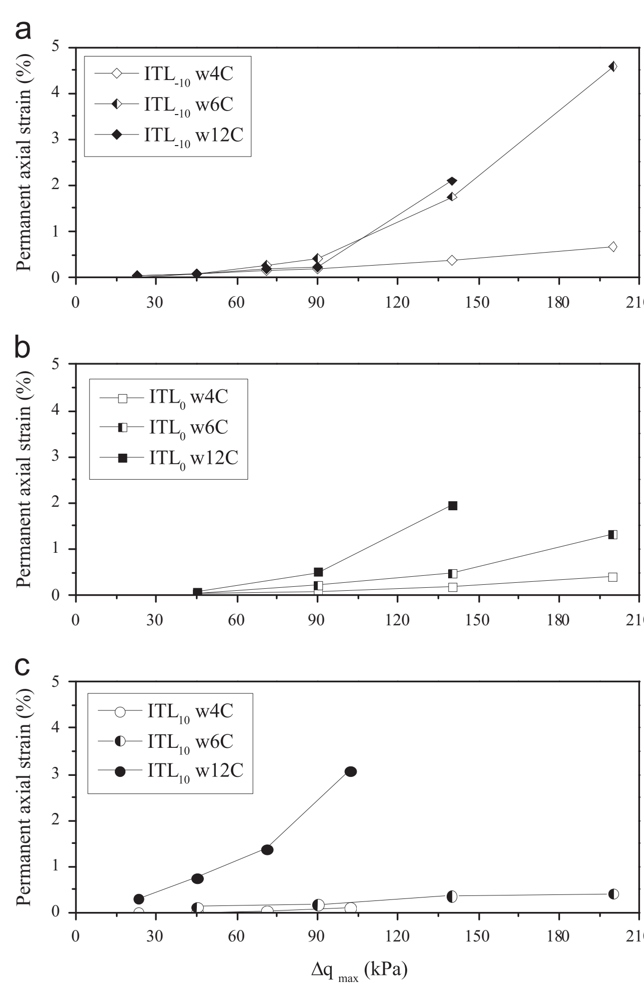


Fig. 13. Effect of water content on the end-stage permanent axial strain for $ITL_{-10}$, $ITL_0$ and $ITL_{10}$.

well separated. At all stress levels, the higher the water content, the larger the permanent axial strain. Failure was also observed for the nearly saturated specimen at $\Delta q_{max}=200$ kPa. For $ITL_{10}$ (Fig. 13c), the curve of the specimens at $w=4\%$ and 6% are similar, while for the nearly saturated specimen ($ITL_{10}w12C$), the permanent axial strain is much larger. The effect of water content depends not only on the soil nature but also on the variation range of water content. Changing the water content from 4% to 6% did not significantly affect the permanent axial strain of $ITL_{10}$, which had the highest fines content but rather induced significant changes in the case of lower fines content ($ITL_{-10}$ and $ITL_0$). On the contrary, increasing the water content from 6% to 12% induced a significant change in the permanent axial strain for $ITL_{10}$ (with the highest fines content), but not for $ITL_{-10}$ (having the lowest fines content) when the stress was lower than 140 kPa. At a given stress level, increasing water content resulted in an increase in permanent axial strain. These permanent axial strains are presented in Fig. 14 showing the influence of degree of saturation under difference applied deviator stresses. The influence of water content can be then depicted more clearly. In the case of $ITL_{10}$ (Fig. 14c), when the deviator stress was lower than 90 kPa, a small decrease trend was observed within a small axial strain range ($<5\times10^{-3}$) when the degree of saturation increased from 49% (6% water content) to 100% (12% water content). When the applied stress became higher, the axial strain increased with the increase of degree of saturation (water content) as in other cases (Fig. 14a and b).

Fig. 15 shows the permanent axial strains obtained at the end of each loading step versus the corresponding $q_{max}$ for each water content value, allowing the effect of fines content on the permanent axial strain to be analyzed. In the case of $w=4\%$ and 6% (Fig. 15a and b, respectively), the permanent axial strain for test $ITL_{-10}w4C$ and $ITL_{-10}w6C$ was significantly higher than for others, suggesting that the lower the fines content, the larger the permanent axial strain. In the nearly saturated state (Fig. 15c), the effect of fines content was inversed: the soil with the highest fines content ($ITL_{10}$) exhibited the largest permanent axial strain. Uthus et al. (2005) and Uthus (2007) also observed that the effect of water content on the permanent axial strain depended on the fines content. This phenomenon can be explained as follows: in the unsaturated state, water is mainly trapped by fine particles. At the same density and water content, if the fines content is higher, the soil suction must be higher. As a result, the soil is mechanically more resistant. On the other hand, fine particles are well known to be very sensitive to changes in water content, and when the water content is 12%, the soil becomes saturated and its suction approaches zero leading to a decrease in fine particles strength and further the overall mechanical behavior of soil. Similar observations were reported by Fortunato et al. (2010), Seif El Dine et al. (2010) and Huang et al. (2009).

On the whole, at a given water content in dry condition, adding more fines has a positive effect on the mechanical behavior of interlayer soil (the permanent axial strain is reduced), while in the

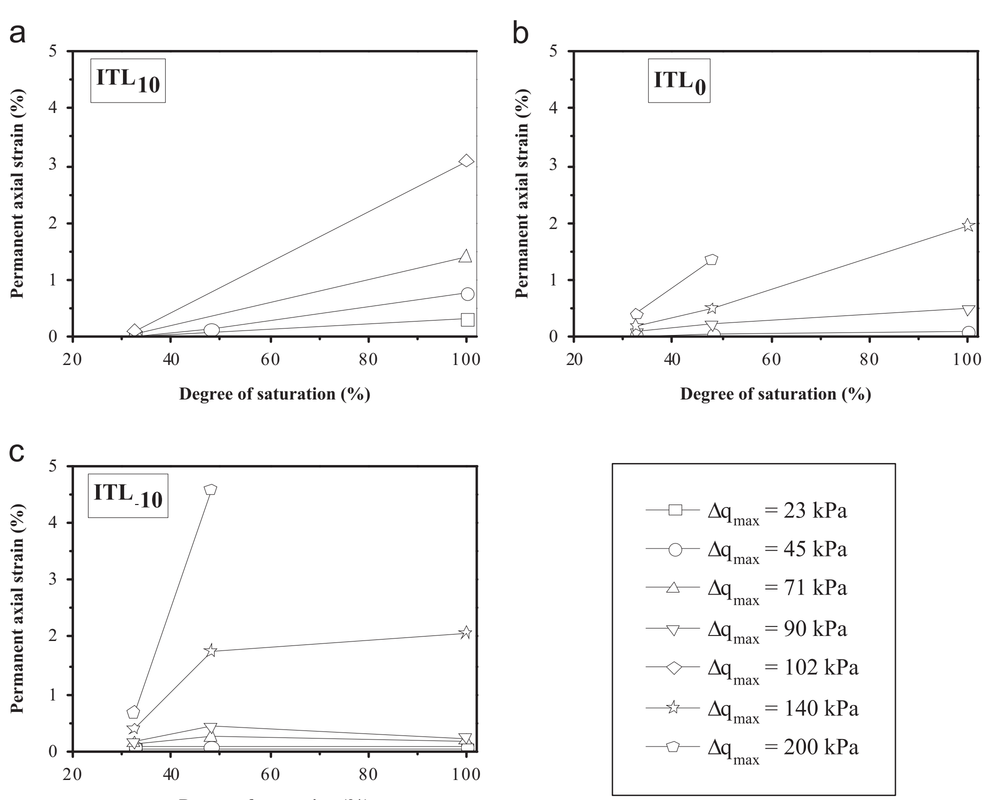


Fig. 14. Water effect with different stress value (a) $ITl_{10}$; (b) $ITl_0$ and (c) $ITl_{-10}$.

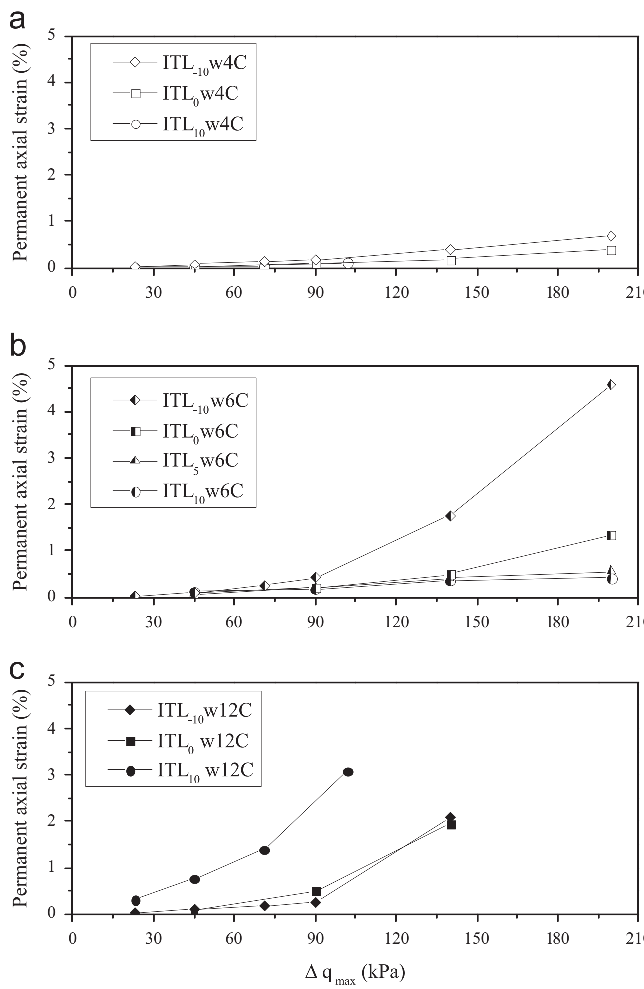


Fig. 15. Effect of fines content on the end-stage permanent axial strain at various water contents.

nearly saturated condition, adding more fines boosts the axial strain. This means that in the railway context, during the assessment and exploitation of the interlayer soil, the effect of water content and fines content must be taken into account together. The interlayer soil containing a larger quantity of fine particles has to be protected from water infiltration in order to avoid any increase of water content that would decrease its mechanical performance.

## 5. Conclusion

The present work investigates the effects of water content and fines content on the mechanical behavior of interlayer soil. The quantity of fine particles in soil was modified by adding/removing fines. Four materials with different fines contents were tested using a large-scale triaxial cell. Monotonic triaxial tests were first performed to study the variation of internal friction angle and cohesion and to help define the deviator stress levels in cyclic triaxial tests. Cyclic triaxial tests were conducted at different water contents and deviator stress levels. The permanent axial strain was investigated to analyze the effects of water and of fine particle contents.

The monotonic triaxial tests showed that increasing water content decreases the shear strength of interlayer soil at two fines contents corresponding to two fouling indices ($FI=45$ and 59). In addition, the effect of water content is more pronounced in the case of higher fine content. Adding more fine particles does not result in a clear change in mechanical properties (friction angle and cohesion) in unsaturated condition ($w=4\%$) but results in significant decrease in nearly saturated condition.

Adding more fine particles affects the cyclic behavior of interlayer soil in different fashions. In dry condition ($w=4\%$ and 6%), adding fines decreases the permanent axial strain due to the suction effect. On the contrary, in nearly saturated condition ($w=12\%$), the higher the fines content the higher the axial permanent strain. This is because the interlayer soil is weakened mechanically due to the sensitivity of fine particles to water content changes in the nearly saturated condition.

From a practical point of view, the increase of fines content on the mechanical behavior of interlayer is acceptable in the case of lower water content (dry state). However, in the case of high water content (at the nearly saturated state), the interlayer with high fines content needs to be protected from water infiltration. Otherwise, a significant decrease in mechanical performance can be expected.

## Acknowledgments

The present work is part of the French national project namely RUFEX (Re-use of ancient railway platforms and existing foundations). The supports from French Railway Company (SNCF) and Ecole des Ponts ParisTech are also gratefully acknowledged.

## References

AFNOR, 2005. XP CEN ISO/TS 17892-9: Geotechnical Investigation and Testing, Laboratory Testing of Soil—Part 9: Consolidated Triaxial Compression Tests on Water-saturated Soils.

Alias, J., 1984. La voie ferrée. Techniques de construction et d'entretien, 2nd ed. Eyrolles Paris, France (in French).

Alobaidi, I., Hoare, D., 1994. Factors affecting the pumping of fines at the subgrade—subbase interface of highway pavements. A laboratory study. Geosynth. Int. 1 (2), 221–259.

Alobaidi, I., Hoare, D., 1996. The development of pore water pressure at the sub-grade-subbase interface of a highway pavement and its effect on pumping of fines. Geotext. Geomembr. 14, 111–135.

Alobaidi, I., Hoare, D., 1998a. The role of geotextile reinforcement in the control of pumping at the sub-grade-subbase interface of highway pavements. Geosynth. Int. 5 (6), 619–636.

Alobaidi, I., Hoare, D., 1998b. Quantitative criteria for anti-pumping geocomposites. Geotext. Geomembr. 16, 221–245.

Alobaidi, I., Hoare, D., 1999. Mechanisms of pumping at the subgrade-subbase interface of highway pavements. Geosynth. Int. 6 (4), 241–259.

Anbazhagan, P., Lijun, S., Buddhima, I., Cholachat, R., 2011. Model track studies on fouled ballast using ground penetrating radar and multichannel analysis of surface wave. J. Appl. Geophys. 74 (4), 175–184.

Ayres, D., 1986. Geotextiles or geomembranes in track? British railways' experience. Geotext. Geomembr. 3 (2–3), 129–142.

Babic, B., Prager, A., Rukavina, T., 2000. Effect of fine particles on some characteristics of granular base courses. Mater. Struct. 33 (7), 419–424.

Bailey, B., Hutchinson, D., Gordon, D., Siemens, G., Ruel, M., 2011. Field and Laboratory Procedures for Investigating the Fouling Process within

Railway Track Ballast. In: Proceeding of the 2011 Pan-Am CGS Geotechnical Conference, 8 pp.
Cabalar, A., 2008. Effect of fines content on the behavior of mixed specimens of a sand. Electron. J. Geotech. Eng. 13 (D), 1–11.
Cabalar, A., 2011. The effects of fines on the behaviour of a sand mixture. Geotech. Geol. Eng. 29 (1), 91–100.
Calon, N., Trinh, V., Tang, A., Cui, Y., Dupla, J., Canou, J., Lambert, L., Robinet, A., Schoen, O., 2010. Caractérisation hydromécanique des matériaux constitutifs de plateformes ferroviaires anciennes. In: Proceeding of the Conference JNGG2010, Grenoble, France, pp. 787–794 (in French).
Cui, Y.J., Delage, P., 1996. Yielding and plastic behaviour of an unsaturated compacted silt. Géotechnique 46 (2), 291–311.
Dupla, J.-C., Pedro, L.S., Canou, J., Dormieux, L., 2007. Mechanical behaviour of coarse grained soils reference. Bull. Liaison Lab. Ponts Chaussées 268–269, 31–58.
Duong, T.V., Trinh, V.N., Cui, Y.J., Tang, A.M., Calon, N., 2013. Development of a large-scale infiltration column for studying the hydraulic conductivity of unsaturated fouled ballast. Geotech. Test. J. 36 (1), 1–10. http://dx.doi.org/10.1520/GTJ20120099.
Ebrahimi, A., 2011. Behavior or fouled ballast. Railw. Track Struct. 107 (8), 25–31.
Fortunato, E., Pinelo, A., Matos Fernandes, M., 2010. Characterization of the fouled ballast layer in the sub-structure of a 19th century railway track under renewal. Soils Found. 50 (1), 55–62.
Ghataora, G., Burns, B., Burrow, M., Evdorides, H., 2006. Development of an Index Test for Assessing Anti-pumping Materials in Railway Track Foundations. In: Proceeding of the First International Conference on Railway Foundations, pp. 355–366.
Giannakos, K., 2010. Loads on track, ballast fouling, and life cycle under dynamic loading in railways. J. Transp. Eng. 136 (12), 1075–1084.
Gidel, G., Hornych, P., Chauvin, J.J., Breysse, D., Denis, A., 2001. A new approach for investigating the permanent deformation behavior of unbound granular material using the Repeated Load Triaxial Apparatus. Bull. Liaison Lab. Ponts Chaussées 233, 5–21.
Grabe, P., Clayton, C., 2009. Effects of principal stress rotation on permanent deformation in rail track foundations. J. Geotech. Geoenviron. Eng. 135 (4), 555–565.
Huang, H., Tutumluer, E., Dombrow, W., 2009. Laboratory characterization of fouled railroad ballast behavior. J. Transp. Res. Board 2117 (1), 93–101. http://dx.doi.org/ 10.3141/2117-12.
Inam, A., Ishikawa, T., Miura, S., 2012. Effect of principal stress axis rotation on cyclic plastic deformation characteristics of unsaturated base course material. Soils Found. 52 (3), 465–480.
Indraratna, B., Ionescu, D., Christie, H.D., 1998. Shear behavior of railway ballast based on large-scale triaxial tests. J. Geotech. Geoenviron. Eng. 124 (5), 439–449.
Indraratna, B., Salim, W., 2002. Modelling of Particles Breakage of Coarse Aggregates Incorporating Strength and Dilatancy. In: Proceedings of the ICE—Geotechnical Engineering, vol. 155(4), pp. 243–252.
Indraratna, B., Su, L., Rujikiatkamjorn, C., 2011a. A new parameter for classification and evaluation of railway ballast fouling. Can. Geotech. J. 48 (2), 322–326.
Indraratna, B., Salim, W., Rujikiatkamjorn, C., 2011b. Advanced Rail Geotechnology—Ballasted Track. CRC Press, London, UK 413 pp.
Jain, V., Keshav, K., 1999. Stress Distribution in Railway Formation—A Simulated Study. In: Proceeding of the 2nd International Symposium on Pre-Failure Deformation Characteristics of Geomaterials—IS Torino. pp. 653–658.
Kim, D., Sagong, M., Lee, Y., 2005. Effects of fine aggregate content on the mechanical properties of the compacted decomposed granitic soils. Constr. Build. Mater. 19 (3), 189–196.
LCPC, SETRA, 2000. Technical Guidelines on Embankment and Capping Layers Construction, GTR.
Li, D., Selig, E., 1998. Method for railroad track foundation design. I. Development. J. Geotech. Geoenviron. Eng. 124 (4), 316–322.
Lieberenz, K., Piereder, F., 2011. Track sub-structure improvements to increase load-bearing strength. Rail Eng. Int. 40 (4), 6–10.
Mayoraz, F., Vulliet, L., Laloui, L., 2006. Attrition and particle breakage under monotonic and cyclic loading. Comp. R. Méc. 334 (1), 1–7.
Naeini, S., Baziar, M., 2004. Effect of fines content on steady-state strength of mixed and layered specimens of a sand. Soil Dyn. Earthq. Eng. 24 (3), 181–187.
Pedro, L., 2004. De l'étude du comportement mécanique de sols hétérogènes modèles à son application au cas des sols naturels (Ph.D. dissertation). Ecole Nationale des Ponts et Chaussées, France (in French).
Read, D., Hyslip, J., McDaniel, J., 2011. Heavy Axle Load Revenue Service Mud-fouled Ballast Investigation, Technical Report. Federal Railroad Administration. U.S. Department of Transportation.
Seif El Dine, S., Dupla, J., Frank, R., Canou, J., Kazan, Y., 2010. Mechanical characterization of matrix coarse-grained soils with a large-sized triaxial device. Can. Geotech. J. 47 (4), 425–438.
Selig, E., Waters, J., 1994. Track Geotechnology and Sub-structure Management. Thomas Telford, London, UK 450 pp.
SNCF, 2009. Sollicitations mécaniques dans la plate-forme. Mesures d'accélérations verticales dans la plate-forme. Technical Report R2520-2009-01 (in French).
Sussmann, T. R.; Ruel, M., Christmer, S., 2012. Sources, Influence, and Criteria for Ballast Fouling Condition Assessment. In: Proceeding of the 91st Annual Meeting of the Transportation Research Board, 11 pp.
Taheri, A., Tatsuoka, F., 2012. Stress–strain relations of cement-mixed gravelly soil from multiple-step triaxial compression test results. Soils Found. 52 (4), 748–766.
Trinh, V.N., Tang, A.M., Cui, Y.J., Dupla, J.C., Canou, J., Calon, N., Lambert, L., Robinet, A., Schoen, O., 2010a. Calibration of Smart Irrigation Sensor (sis-ums) for the Blanket Layer Soil from old Railway Lines. Proceeding of the Conference UNSAT2010, Barcelone, Espagne, pp. 739–744.
Trinh, V.N., Tang, A.M., Cui, Y.J., Dupla, J.C., Canou, J., Calon, N., Lambert, L., Robinet, A., Schoen, O., 2010b. Unsaturated Hydraulic Properties of Fines-grained Soil from the Blanket Layer of old Railway Lines in France. In: Proceeding of the Conference UNSAT2010, Barcelone, Espagne, pp. 501–507.
Trinh, V., 2011. Comportement hydromécanique des matériaux constitutifs de plateformes ferroviaires anciennes (Ph.D. dissertation). Ecole Nationale des Ponts et Chaussées – Université Paris – Est, France (in French).
Trinh, V.N., Tang, A.M., Cui, Y.J., Dupla, J.C., Canou, J., Calon, N., Lambert, L., Robinet, A., Schoen, O., 2011a. Caractérisation des matériaux constitutifs de plate-forme ferroviaire ancienne. Rev. Fr. Géotech. 134–135, 65–74 (in French).
Trinh, V.N., Tang, A.M., Cui, Y.J., Dupla, J.C., Canou, J., Calon, N., Lambert, L., Robinet, A., Schoen, O., 2011b. Caractérisation hydromécanique des matériaux constitutifs de plateformes ferroviaires anciennes. In: Proceeding of the International Symposium Georail 2011, Paris, France, pp. 377–387 (in French).
Trinh, V.N., Tang, A.M., Cui, Y.J., Dupla, J.C., Canou, J., Calon, N., Lambert, L., Robinet, A., Schoen, O., 2012. Mechanical characterisation of the fouled ballast in ancient railway track sub-structure by large-scale triaxial tests. Soils Found. 52 (3), 511–523. http://dx.doi.org/10.1016/j.sandf.2012.05.009.
Uthus, L., 2007. Deformation Properties of Unbound Granular Aggregate (Ph. D. dissertation). Norwegian University of Science and Technology, Norway.
Uthus, L., Hoff, I., Horvli, I., 2005. A Study on the Influence of Water and Fines on the Deformation Properties of Unbound Aggregates. In: Proceeding of the 7th International Conference on the Bearing Capacity of Roads, Railways and Airfields. Trondheim, Norway, pp. 1–13.
Verdugo, R., Hoz, K., 2007. Strength and stiffness of coarse granular soils. Solid Mech. Appl. 146 (3), 243–252.
Voottipruex, P., Roongthanee, J., 2003. Prevention of mud pumping in railway embankment, a case study from Baeng pra-pitsanuloke, Thailand. J. KMITB 13 (1), 20–25.
Vilhar, G., Jovicic, V., Coop, M.R., 2013. The role of particle breakage in the mechanics of a non-plastic silty sand. Soils Found. 53 (1), 91–104.
Wang, Q., Tang, A.M., Cui, Y.J., Delage, P., Barnichon, J.D., Ye, W.M., 2013. The effects of technological voids on the hydro-mechanical behaviour of compacted bentonite–sand mixture. Soils Found. 53 (2), 232–245.
Yang, L., Powrie, W., Priest, J., 2009. Dynamic stress analysis of a ballasted railway track bed during train passage. J. Geotech. Geoenviron. Eng. 135 (5), 680–689.
Zeghal, M., 2009. The impact of grain crushing on road performance. Geotech. Geol. Eng. 27 (4), 549–558.